Multi-Aspect Micro-Doppler Signatures for Attitude-Independent *L*/*N* Quotient Estimation and its Application to Helicopter Classification

Rui Zhang [1], Gang Li [1*], Carmine Clemente [2], John J. Soraghan [2]

[1] Department of Electronic Engineering, Tsinghua University, Beijing, China
[2] Department of Electronic and Electrical Engineering, University of Strathclyde, 204 George Street, G1 1XW, Glasgow, UK
[*]gangli@tsinghua.edu.cn

Abstract: Micro-Doppler signals returned from the main rotor of a helicopter can be used for feature extraction and helicopter classification. An intrinsic feature of a helicopter that may be extracted from the micro-Doppler signatures is the *L*/*N* quotient, where *N* denotes the number of rotor blades and *L* is the blade length. However, in monostatic radar, the *L*/*N* quotient cannot be accurately estimated due to the unknown attitude angles of non-cooperative helicopters. To solve this problem, an attitude-independent *L*/*N* quotient estimation method based on multi-aspect micro-Doppler signatures is proposed in this paper. The helicopter is observed from different aspect angles, and the multi-aspect micro-Doppler signatures are jointly processed to solve the attitude angles of the helicopter and estimate the *L*/*N* quotient unambiguously. Experiments with both simulated and real data demonstrate that, the proposed method is robust with respect to the attitude of the helicopter and, therefore, significantly improves the accuracy of *L*/*N* quotient estimation compared to only using the signature observed from single-aspect angle. This implies that the proposed method has the potential to increase the success rate of helicopter classification.

1. Introduction

Micro-Doppler signatures induced by the mechanical vibration or rotation of a target or its parts have been widely exploited for civil and military purposes [1-7]. In recent years, the problem of micro-Doppler-based helicopter classification has attracted much attention because of its application in air defence systems [8-18]. The *L*/*N* quotient, where *N* denotes the number of rotor blades and *L* is the blade length, is an intrinsic feature of a helicopter and has been widely used for helicopter classification. In [10-13], the authors developed the *L*/*N* quotient-based helicopter classification algorithm using monostatic radar. These methods can accurately identify the helicopter type in the assumption that the attitude of helicopter is horizontal. However, for non-cooperative helicopters with unknown attitudes, the methods in [10-13] suffer from performance degradation, because the *L*/*N* quotient solved by a monostatic radar is sensitive to the attitude of the helicopter. In practical applications, the main rotor of a helicopter has different attitudes due to the change of helicopter motion such as hovering, advancing and retreating [14, 15]. Therefore, the attitude-independent *L*/*N* quotient estimation is meaningful in practical scenarios and helpful to improve the robustness of existing algorithms of helicopter classification [16-19].

In order to overcome the limitation of monostatic radar, bistatic and multistatic radars have been employed to micro-Doppler-based target classification [20-29]. In [20-22], the motion parameters of vibrating/rotating targets were extracted based on analytical signal models in multistatic radar systems. In [23-26], the multistatic micro-Doppler signatures were used to overcome the self-occlusion of human target and obtain satisfactory classification results when the movement of the human target is away from the line of sight (LOS) of radar. However, these methods proposed in [23-26] cannot be straightforwardly applied in helicopter classification due to the distinct difference between the motion properties of helicopters and personnel targets. More specifically, the principal axis of a human is approximately perpendicular (when the human is walking or running) or parallel (when the human is crawling) to the ground, while the rotation axis of helicopter rotor has more variations in different helicopter motions such as hovering, advancing and retreating [14, 15].

Multistatic or multi-aspect micro-Doppler signatures of helicopter have attracted much attention in recent years [27-29]. In [27], the Global Navigation Satellite System (GNSS) is employed as the illuminator of a passive bistatic radar system to observe helicopters, and theoretical analysis and simulations demonstrate the effectiveness of this system for extracting helicopter signatures. In [28], multiple-input multiple-output (MIMO) radar is used to detect helicopters and the detection performance is effectively improved in comparison with monostatic radar. In [29], the authors formulated the signal model of the helicopter rotor in multistatic passive radars, which allow both estimation of helicopter parameters and inverse synthetic aperture radar (ISAR) imaging of the helicopter rotor. However, in existing literature, the effect of the attitude of the helicopter on the feature extraction has not been fully investigated yet.

In this paper, an attitude-independent L/N quotient estimation method is proposed based on multi-aspect micro-Doppler signatures. Based on the analytical relationship between the maximal micro-Doppler shift and the helicopter attitude, the attitude angles of the helicopter can be solved by analysing the micro-Doppler signatures collected from multiple aspect angles, and then the L/N quotient can be accurately retrieved and used for helicopter classification. Compared to the existing monostatic-based methods in [10-13] that do not consider the helicopter attitude, the proposed algorithm can provide satisfactory classification performance for non-cooperative helicopters with unknown attitudes.

The remainder of the paper is organized as follows. In Section 2, the background related to micro-Doppler signal model and helicopter classification is introduced. Then the proposed method is presented in detail in Section 3. Experimental results on synthetic and real data are given in Section 4 to validate the proposed method. Concluding remarks are provided in Section 5.

2. Background

2.1. Signal Model of Rotor Echo

The helicopter's echoes are composed of the components reflected from its fuselage, rotating main rotor hub, main rotor and tail rotor [8, 9]. From the point of view of helicopter classification, the most useful information is provided by the structure of the rotating main rotor [12, 18], and the main rotor echoes can be separated from other components by using the method proposed in [18]. Supposing the parameters (N, ω, L) represent the number of blades, the rotational speed and the blade length, respectively, the echoes from the main rotor can be expressed as [19]:

$$y(t_m) = \sigma L \exp\left(-j\frac{4\pi R_0}{\lambda}\right) \times \sum_{n=0}^{N-1} \mathrm{sinc}\left[\Phi_n(t_m)\right] \exp\left[-j\Phi_n(t_m)\right] \ , \ m = 0,1,...,M-1, \tag{1}$$

where

$$\Phi_n(t_m) = \frac{4\pi L}{\lambda} \sin\varphi_{rot,los} \times \cos\left(\omega t_m + \frac{2\pi n}{N} + \theta\right), \tag{2}$$

λ is the carrier wavelength of the radar system, t_m denotes the sampling instant with the sampling frequency f_s, M is the number of samples, $\mathrm{sinc}(x) = \sin(x)/x$, R_0 is the range between the helicopter and the radar, σ is the equivalent scattering coefficient of the main rotor, and $\Phi_n(t_m)$ denotes the phase of the echo corresponding to the n-th blade, θ denotes the initial phase of the received signal, $\varphi_{rot,los}$ is the angle formed by the rotation axis and the LOS direction. In (2), the sine of angle $\varphi_{rot,los}$ follows

$$\sin\varphi_{rot,los} = \sqrt{1 - \left\langle \boldsymbol{\eta}_{rot}, \boldsymbol{\eta}_{los} \right\rangle^2}, \tag{3}$$

where the vector $\boldsymbol{\eta}_{rot}$ denotes the direction of the rotation axis, $\boldsymbol{\eta}_{los}$ denotes the LOS direction, and $< , >$ denotes the inner product. The geometry of radar observation is shown in Fig. 1, where α_{rot} and β_{rot} denote the azimuth angle and the pitch angle of $\boldsymbol{\eta}_{rot}$, respectively, α_{los} and β_{los} denote the azimuth angle and the pitch angle of $\boldsymbol{\eta}_{los}$, respectively. Then $\boldsymbol{\eta}_{rot}$ and $\boldsymbol{\eta}_{los}$ can be expressed as

$$\boldsymbol{\eta}_{rot} = \left(\cos\alpha_{rot}\cos\beta_{rot},\ \sin\alpha_{rot}\cos\beta_{rot},\ \sin\beta_{rot}\right), \tag{4}$$

$$\boldsymbol{\eta}_{los} = \left(\cos\alpha_{los}\cos\beta_{los},\ \sin\alpha_{los}\cos\beta_{los},\ \sin\beta_{los}\right). \tag{5}$$

In practical scenarios, the LOS angles (α_{los}, β_{los}) can be obtained from system configuration or estimated by using signal processing techniques [30], but the attitude angles (α_{rot}, β_{rot}) of non-cooperative helicopters are unknown [14, 15]. Since the micro-Doppler signatures are influenced by the helicopter attitude, it is very meaningful to develop attitude-independent algorithms of helicopter feature extraction in practical scenarios.

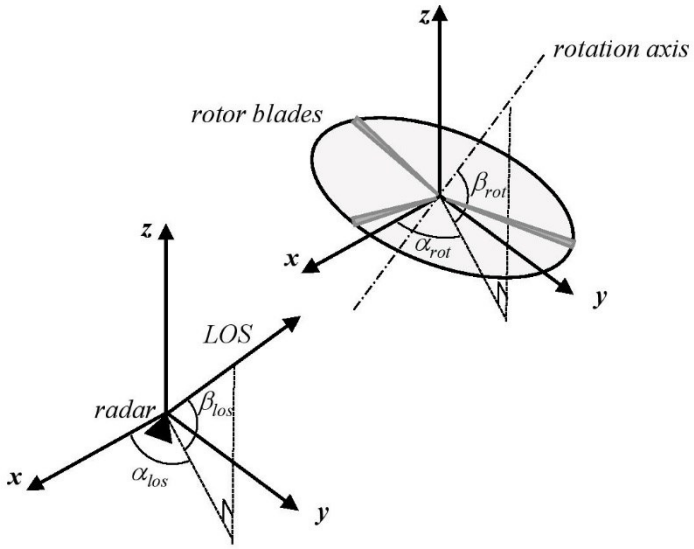

Fig. 1. *Geometry of a radar and a 3-blade rotor.*

2.2. L/N Quotient-based Classification Scheme

The *L*/*N* quotient-based algorithm is one of the most widely used methods for helicopter classification [10-13]. In this subsection, the theoretical foundation of this method is briefly reviewed, and its limitation in monostatic scenario is also analysed.

It is clear from (1) and (2) that the received signal is periodic and the period is

$$T = \frac{2\pi}{N\omega}. \tag{6}$$

The instantaneous frequency corresponding to the *n*-th blade can be directly obtained by taking the time derivative of $\Phi_n(t)$:

$$\begin{aligned} f_{md,n}\left(t_m\right) &= \frac{1}{2\pi} \times \frac{d\Phi_n\left(t\right)}{dt} \\ &= -\frac{2}{\lambda}\omega L \sin\varphi_{rot,los} \times \sin\left(\omega t_m + \frac{2\pi n}{N} + \theta\right), \end{aligned} \tag{7}$$

It is obvious from (7) that the maximal Doppler shift of the received signal is

$$f_{md,\max} = \frac{2}{\lambda}\omega L \sin\varphi_{rot,los}. \tag{8}$$

According to (6) and (8), the *L*/*N* quotient can be calculated as

$$\begin{aligned} \frac{L}{N} &= \frac{\lambda}{4\pi} \times \frac{Tf_{md,\max}}{\sin\varphi_{rot,los}} \\ &= \frac{\lambda}{4\pi} \times \frac{Tf_{md,\max}}{\sqrt{1-\left\langle \boldsymbol{\eta}_{rot}, \boldsymbol{\eta}_{los} \right\rangle^2}} \quad . \end{aligned} \tag{9}$$

where the period T and maximal Doppler shift $f_{md,max}$ can be extracted from the micro-Doppler signals. Since L/N quotient is an intrinsic characteristic of a helicopter, most helicopters can be identified according to their L/N quotient values [16].

In monostatic-based algorithm, no information about the helicopter attitude can be obtained and the helicopter pitch angle β_{rot} is assumed to be 90°. As a result, the L/N quotient is regarded as

$$\left(\frac{L}{N}\right)_{mono} = \frac{\lambda}{4\pi} \times \frac{Tf_{md,\max}}{\cos\beta_{los}} \ . \tag{10}$$

It is obvious that formula (10) is different from (9), and the estimated $(L/N)_{mono}$ will deviate from the real value of L/N quotient when the helicopter attitude is not horizontal. That is to say, the monostatic-based algorithm cannot accurately estimate the L/N quotient of non-cooperative helicopters with unknown attitudes.

Table 1 The parameters in the example in Section 2.2

Carrier frequency f_c	900 MHz
Sampling frequency f_s	6 KHz
Sampling number M	2400
Rotor attitude angles (α_{rot}, β_{rot})	(60°, 75°)
LOS angles (α_{los}, β_{los})	(0°, 40°)

Table 2 The parameters of helicopter.

Type	N	L (m)	ω (rps)	L/N	* range of β_{rot}
AH-1 Cobra	2	7.32	4.9	3.66	[74°, 106°]
AH-64 Apache	4	7.32	4.8	1.83	[60°, 120°]
UH-60 Black Hawk	4	8.18	4.3	2.05	[60°, 120°]
AS332 Super Puma	4	7.80	4.4	1.95	[74°, 106°]
A109 Agusta	4	5.50	6.4	1.38	[77°, 103°]
SA365 Dauphin	4	5.97	5.8	1.49	[75°, 105°]

* The ranges of β_{rot} are found in the pilot's books of corresponding helicopters.

To explain the failure of monostatic L/N quotient estimation for non-horizontal helicopters, we analyse the micro-Doppler signature of an AH-64 Apache helicopter with the following simulation. The simulation parameters and the parameters of AH-64 Apache helicopter are listed in Table 1 and Table 2, respectively. With the monostatic L/N quotient estimation algorithm, the value of $(L/N)_{mono}$ is calculated as 1.658 when the pitch angle β_{rot} of the rotation axis is 75°, i.e., when the helicopter rotor deviates from the horizontal attitude with 15°. It is clear that $(L/N)_{mono}$ has deviated from the real value of L/N, i.e. 1.830. Considering that the L/N quotient of SA365 Dauphin helicopter (another helicopter type) is 1.490, the AH-

64 Apache with β_{rot} =75° may be mistakenly identified as a SA365 Dauphin by using monostatic L/N quotient estimation according to the nearest neighbour rule.

3. Proposed method

In order to accomplish attitude-independent classification of non-cooperative helicopters, in this section we propose a multi-aspect micro-Doppler-based algorithm for L/N quotient estimation. The block diagram of the proposed method is depicted in Fig. 2. It can be seen that the proposed method can be divided into two stages: 1) monostatic micro-Doppler analysis; 2) Multi-aspect micro-Doppler analysis. The procedures of Stages 1 and 2 are presented in details in the following subsections.

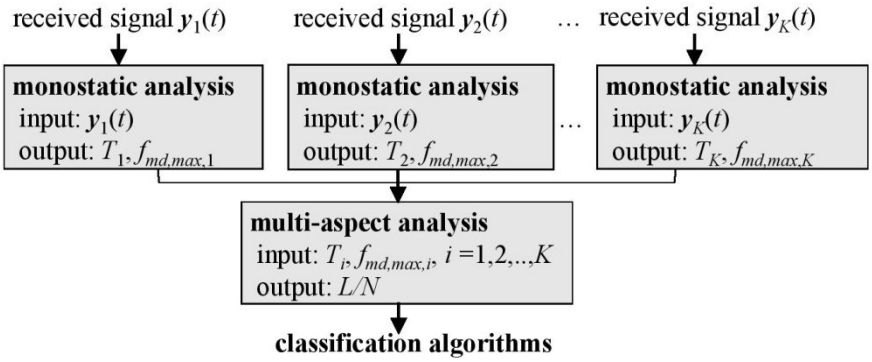

Fig. 2. *The block diagram of the proposed method.*

3.1. Monostatic Micro-Doppler Analysis

At this stage, the received signal obtained from each aspect is processed separately, and the period T_i and maximal Doppler shift $f_{md,\max,i}$ are extracted via monostatic micro-Doppler analysis, where the subscript i indicates the index of aspect. The authors of [10-19] presented a number of effective methods for monostatic micro-Doppler analysis. In this paper, the period T_i is estimated by using the autocorrelation function of the received signal as presented in [18]. Then, the initial phase θ of the received signal is synchronized to be $\pi/2$ by using the method proposed in [19]. After the previous processing, the signal model in (1) can be rewritten as

$$y_{N,f_{md,\max}}(t_m) = C \times \sum_{n=0}^{N-1} \left\{ \operatorname{sinc}\left\{ -TNf_{md,\max} \sin\left[\frac{2\pi}{N}\left(\frac{t_m}{T} + n \right) \right] \right\} \times \exp\left\{ jTNf_{md,\max} \sin\left[\frac{2\pi}{N}\left(\frac{t_m}{T} + n \right) \right] \right\} \right\}, \quad \textbf{(11)}$$

where C is a constant, and the rotational speed ω is replaced with $2\pi/NT$ according to (6).

For each parameter pair $(N, f_{md,max}) \in \{2,3,\ldots,7\} \otimes (0, f_s/4]$, the following correlation coefficient measures the relevancy between the model $y_{N,fmd,max}(t_m)$ and the received signal $y(t_m)$:

$$c_{N,f_{md,\max}} = \frac{\sum_{m=0}^{M-1} y_{N,f_{md,\max}}(t_m)\, y^*(t_m)}{\sqrt{\sum_{m=0}^{M-1} \left| y_{N,f_{md,\max}}(t_m) \right|^2 \sum_{m=0}^{M-1} \left| y(t_m) \right|^2}}, \tag{12}$$

Based on the Maximum Likelihood (ML) analysis presented in [18], the maximal Doppler shift $f_{md,max}$ can be estimated as:

$$f_{md,\max} = \arg\max_{f_{md,\max} \le f_s/4} \left\{ \max_{N \in \{2,3,\ldots,7\}} c_{N,f_{md,\max}} \right\} . \tag{13}$$

It is worth emphasizing that the maximal Doppler shift $f_{md,max}$ can be properly extracted according to (14) without a priori information about the number of blades N. We refer readers to literature [18] for more details about this maximum likelihood estimation.

3.2. The Multi-Aspect Micro-Doppler Analysis Algorithm

At this stage, the attitude angles (α_{rot}, β_{rot}) are determined by using the maximal Doppler shift $f_{md,\max,i}$ and the LOS angles ($\alpha_{los,i}$, $\beta_{los,i}$) (i =1,2,…,K). Then, with the estimated attitude angles (α_{rot}, β_{rot}), we can calculate the L/N quotient according to (9). The multi-aspect micro-Doppler analysis at this stage accomplishes attitude-independent L/N quotient estimation, which has not been investigated in existing literature yet.

It is clear from (8) that the maximal Doppler shift $f_{md,\max}$ is proportional to the following three factors: 1) the velocity of the blade tip, i.e. ωL; 2) the reciprocal of the wave length, i.e. $1/\lambda$; and 3) the sine value $\sin\varphi_{rot,los}$. Supposing that the helicopter is observed from K different aspects, the maximal Doppler shifts corresponding to Aspect i and Aspect j satisfy the following relationship according to (8):

$$\frac{f_{md,\max,i}}{f_{md,\max,j}} = \frac{\sin\varphi_{rot,los,i}/\lambda_i}{\sin\varphi_{rot,los,j}/\lambda_j} \ , \ (i,j = 1,2,...,K.) \tag{14}$$

where $\varphi_{rot,los,i}$ denotes the included angle formed by rotation axis of the helicopter rotor and the LOS of Aspect i. To avoid zero term at denominator in (15), which corresponds to the case that the LOS is perpendicular to the rotor plane, (15) is rewritten as:

$$\frac{f_{md,\max,i}}{\sum_{j=1}^{K} f_{md,\max,j}} = \frac{\sin\varphi_{rot,los,i}/\lambda_i}{\sum_{j=1}^{K} \sin\varphi_{rot,los,j}/\lambda_j} \ . \ (i = 1,2,...,K.) \tag{15}$$

In (16), the micro-Doppler shifts $f_{md,\max,i}$ (i = 1, 2,…, K) have been estimated in Stage 1, the angle $\varphi_{rot,los,i}$ is determined by ($\alpha_{los,i}$, $\beta_{los,i}$) and (α_{rot}, β_{rot}), where ($\alpha_{los,i}$, $\beta_{los,i}$) are known and (α_{rot}, β_{rot}) are unknown. Based on (16), a group of constraint equations containing (α_{rot}, β_{rot}) are obtained. Since there

are two independent unknown angles, i.e., α_{rot} and β_{rot}, at least two independent constraint equations are needed to determine them. Therefore, the helicopter should be observed from at least three aspects, i.e., $K \geq 3$.

It is difficult to find the analytical solution of (16). Here we solve the values of (α_{rot}, β_{rot}) by full search. We uniformly divide the attitude angles domain that (α_{rot}, β_{rot}) belong in into $P \times Q$ discrete values, i.e. $\alpha_{rot} \in \{\alpha_1, \alpha_2, \ldots, \alpha_P\}$ and $\beta_{rot} \in \{\beta_1, \beta_2, \ldots, \beta_Q\}$, and compute the sine value $\sin\varphi_{rot,los,i}$ according to (3)-(5) for each pair of (α_{rot}, β_{rot}). Based on (16), the value of (α_{rot}, β_{rot}) is searched by

$$\left(\alpha'_{rot}, \beta'_{rot}\right) = \arg\max_{(\alpha_{rot},\beta_{rot})} \mathrm{X}_K\left(\alpha_{rot}, \beta_{rot}\right) , \tag{16}$$

where

$$\mathrm{X}_K\left(\alpha_{rot}, \beta_{rot}\right) = \sum_{i=1}^{K} \left(\left| \frac{\sin\left[\varphi_i\left(\alpha_{rot}, \beta_{rot}\right)\right]/\lambda_i}{\sum_{j=1}^{K} \sin\left[\varphi_j\left(\alpha_{rot}, \beta_{rot}\right)\right]/\lambda_j} - \frac{f_i}{\sum_{j=1}^{K} f_j} \right| \right)^{-2} , \tag{17}$$

where the number of observation K is not less than 3 as analyzed above.

With the estimated (α_{rot}, β_{rot}), the L/N quotient can be calculated according to (9):

$$\left(\frac{L}{N}\right)_{multi,K} = \frac{1}{K} \sum_{i=1}^{K} \frac{\lambda_i}{4\pi} \frac{T_i f_{md,\max,i}}{\sin\varphi_{rot,los,i}} , \tag{18}$$

where T_i have been estimated at Stage 1. It is clear from (19) that the L/N quotient is calculated by averaging over K radar nodes, therefore, the estimation accuracy of $(L/N)_{multi,K}$ is expected to be improved as the number of aspects angles K increases.

Based on the above description, the proposed algorithm for L/N quotient estimation is summarized below:

Algorithm: Attitude-indepent L/N quotient estimation based on multi-aspect micro-Doppler signatures

Input: $y_1(t)$, $y_2(t)$, …, $y_K(t)$, i.e., the received signals observed from K different aspects.

Stage 1: monostatic micro-Doppler analysis. Do Steps 1-1, 1-2 and 1-3, for i=1, 2, …, K.

Step 1-1: Synchronize $y_i(t)$ at the first flash instant.

Step 1-2: Estimate the period T_i of signal $y_i(t)$ by using its autocorrelation function.

Step 1-3: Estimate the maximal micro-Doppler shift $f_{md,\max,i}$ of signal $y_i(t)$ by maximum likelihood method.

Stage 2: multi-aspect micro-Doppler analysis.

Step 2-1: Calculate attitude angles (α_{rot}, β_{rot}) by using $f_{md,\max,i}$ (i=1,2,…, K) according to (17) and (18).

Step 2-2: Calculate L/N quotient according to (19).

Output: The L/N quotient.

In what follows, we use the proposed method to analyse the simulated signal from an AH-64 Apache helicopter which has been described in Section 2.2. The configuration of the radar system and the helicopter parameters are listed in Table 1. Now we assume that the helicopter is observed from three aspects as listed in Table 3.

Table 3 The LOS angles in simulation in Section 3.2

	$\alpha_{los,i}$	$\beta_{los,i}$
Aspect 1	0°	40°
Aspect 2	50°	50°
Aspect 3	90°	60°

Table 4 Results of monostatic analysis in Simulation in Section 3.2

	T_i (ms)	$f_{md,max,i}$ (Hz)
estimate from Aspect 1	52.2	919
estimate from Aspect 2	52.2	567
estimate from Aspect 3	52.2	419

With the algorithms described in Section 3.1, the period and maximal Doppler shift of the received signal from each aspect are extracted separately, and the results are listed in Table 4. It can be seen that, the estimation of the period T_i (i =1,2,3) is not influenced by the change of the aspect angle, while the maximal micro-Doppler shift f_i (i =1,2,3) varies with the different aspect angles.

With the estimated $f_{md,\max,i}$ and the known ($\alpha_{los,i}$, $\beta_{los,i}$) (i =1,2,3), the function $X_3(\alpha_{rot}, \beta_{rot})$ is computed according to (18) and the search result in (α_{rot}, β_{rot}) domain is depicted in Fig. 3. It is clear that the peak of $X_3(\alpha_{rot}, \beta_{rot})$, i.e. (60°, 75°), is located at the real value of (α_{rot}, β_{rot}). With the estimated (α_{rot}, β_{rot}), the L/N quotient is calculated according to (19), and the result is 1.827, which is very close to the real value of L/N, i.e., 1.830. The estimation error in noise free case is caused by the quantization error in searching process and its influence to the classification results is neglectable in most cases. This simulation depicts the processing procedures of the proposed method and verifies the effectiveness of this method. The performance of the proposed method will be evaluated in detail in Section 4.

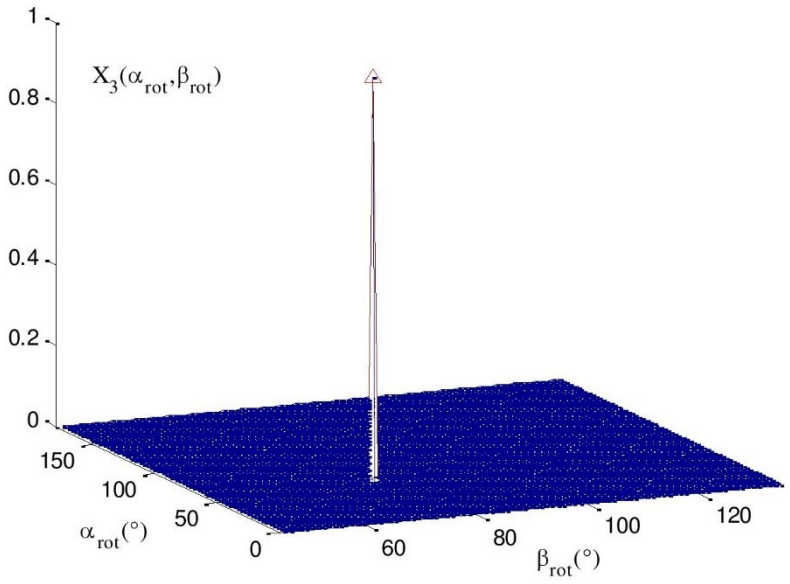

Fig. 3. *The distributions of* $X_3(\alpha_{rot}, \beta_{rot})$*. The red triangle indicates the true values of* $(\alpha_{rot}, \beta_{rot})$*.*

3.3. Discussions

3.3.1 Discussions about the Ranges of Related Angles: In this subsection, the search domain of $(\alpha_{rot}, \beta_{rot})$ and the value ranges of $(\alpha_{los,i}, \beta_{los,i})$ in optimization problem (17) are discussed. Each type of helicopter has its own limitation of pitch angle β_{rot}, and the allowable range of β_{rot} can be found in its pilot's handbook. It can be seen from Table 2 that the deviation of pitch angle β_{rot} from 90° is less than 30°. Therefore, we set the search range of β_{rot} to be [60°, 120°] in (17). Since the azimuth angle α_{rot} of helicopter rotor varies from 0° to 180°, and the azimuth angles between 180° and 360° are equivalent to those between 0° and 180° due to the symmetry of helicopter rotor, we set the search range of α_{rot} to be [0°, 180°]. The range of the pitch angle $\beta_{los,i}$ of the LOS depends on application scenarios. In this paper, the performance of the proposed method is investigated under the following two scenarios: 1) Small pitch angle, i.e. $\beta_{los,i} \in$[0°, 3°]. This scenario is corresponding to applications of classifying helicopters at a remote distance. 2) Wide range of pitch angle, i.e. $\beta_{los,i} \in$[0°, 70°]. This corresponds to more general scenarios. For example, in applications of classifying unmanned micro-Drones in city scenarios [32], the pitch angle of radar LOS can be much larger than 3°. In addition, the azimuth angle $\alpha_{los,i}$ of radar LOS varies between 0° and 360°. In conclusion, the search domain of optimization problem (17) is $(\alpha_{rot}, \beta_{rot}) \in$[0°, 180°] ⊗ [60°, 120°], and the value range of $(\alpha_{los,i}, \beta_{los,i})$ is [0°, 360°] ⊗ [0°, 3°] (in Scenario 1) or [0°, 360°] ⊗ [0°, 70°] (in Scenario 2).

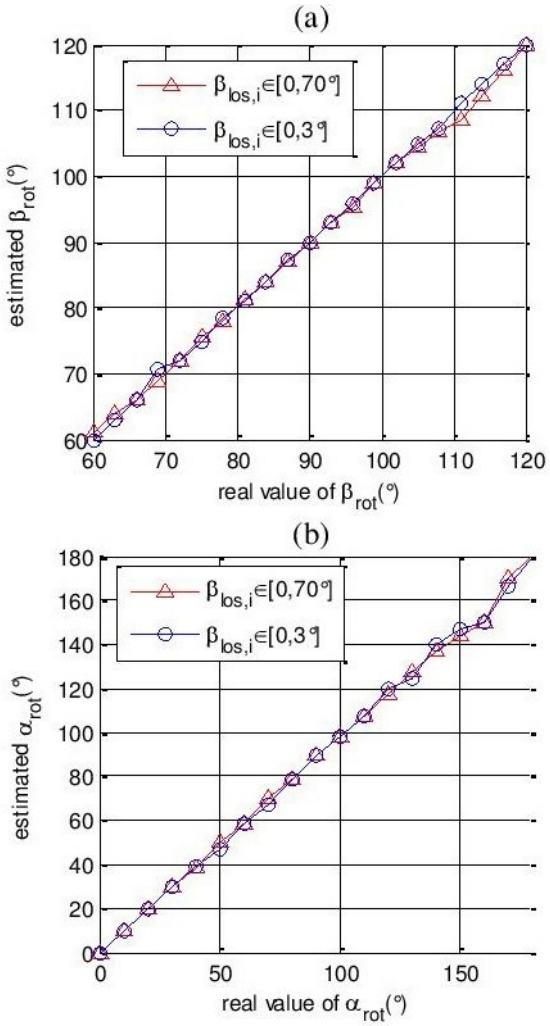

Fig. 4. *The angles (α_{rot}, β_{rot}) estimated by the proposed method versus their real values.*
a estimated β_{rot} versus real value of β_{rot}.
b estimated α_{rot} versus real value of α_{rot}.

3.3.2 Discussions about the Optimization Problem (17): As presented in Section 3.2, the solution of (17) is obtained by full search within search domain of (α_{rot}, β_{rot}). In the searching process, as the angles (α_{rot}, β_{rot}) approach their real values, every term at the right side of (18) approaches $+\infty$. Therefore, the values of (α_{rot}, β_{rot}) can be found by searching the maximum of (17). To evaluate the properties of the optimization problem (17) throughout the search domain of (α_{rot}, β_{rot}), we perform the following simulations with parameters of AH-64 Apache. First, the value of β_{rot} is selected from 60° to 120° with a step size of 3°, and the angles α_{rot}, $\alpha_{los,i}$ and $\beta_{los,i}$ are randomly selected from [0°, 180°], [0°, 360°] and [0°, 3°] (in Scenario 1) or [0°, 70°] (in Scenario 2), respectively. Under each value of β_{rot}, we perform 50 trials of simulations, and the value of estimated β_{rot} is averaged over 50 trials. The relative error of β_{rot}, which is defined as the absolute estimation error of β_{rot} normalized by its real value, is averaged over all trials. The

simulation results are depicted in Fig. 4 (a) and table 5, and the results show that angle β_{rot} can be accurately estimated throughout the value range of β_{rot}. Then, similar simulations are performed to evaluate the estimation accuracy of azimuth angle α_{rot}. The azimuth angle α_{rot} is selected from 0° to 180° with a step size of 10°, and the angles β_{rot}, $\alpha_{los,i}$ and $\beta_{los,i}$ are randomly selected from [60°, 120°], [0°, 360°] and [0°, 3°] (in Scenario 1) or [0°, 70°] (in Scenario 2), respectively. Simulation results depicted in Fig. 4 (b) and Table 5 confirm the effectiveness of the proposed method for estimating α_{rot}. The relative error of α_{rot} is larger than that of β_{rot}, this is because function (18) is more sensitive to the value of β_{rot}.

Table 5 The relative errors of (α_{rot}, β_{rot})

	Scenario 1 $\beta_{los,i}\in[0°, 3°]$	*Scenario 2* $\beta_{los,i}\in[0°, 70°]$
relative error of β_{rot}	0.28%	0.97%
relative error of α_{rot}	3.22%	2.95%

4. Simulations and Experimental Results

In this section, we evaluate the proposed algorithm with both simulated and real data.

4.1. Influence of the Helicopter Attitude on L/N Quotient Estimation in Noise-free Case

As presented in Section 2.2, the monostatic L/N quotient estimation algorithm fails to identify helicopters when the rotor of helicopter deviates from horizontal attitude. In contrast, the proposed method is capable of attitude-independent L/N quotient estimation. In this simulation, the performances of the proposed method and the monostatic L/N quotient estimation are tested under different helicopter attitudes.

The carrier frequency f_c of radar is set to be 900 MHz. The sampling frequency f_s and signal length M are set to be 6000 Hz and 2400 points, respectively. Six types of helicopters are considered and their parameters are listed in Table 2. The helicopter is observed from three different aspects. The azimuth angles $\alpha_{los,i}$ (i = 1,2,3) of the LOS are randomly selected from [0°, 360°] with equal probability. The pitch angles $\beta_{los,i}$ (i = 1,2,3) of the LOS are configured under the following two scenarios: 1) Small pitch angle, i.e. angles $\beta_{los,i}$ (i = 1,2,3) are selected from [0°, 3°] with equal probability. 2) Wide range of pitch angle, i.e. angles $\beta_{los,i}$ (i = 1,2,3) are selected from [0°, 70°] with equal probability. The azimuth angle α_{rot} of the rotor is randomly selected from [0°, 180°] with equal probability, and the pitch angle β_{rot} is set to vary from 75° to 105° with a step size of 2.5°. For each value of β_{rot}, the proposed method and the monostatic L/N quotient estimation algorithm are repeated for 100 trials for each type of helicopter. In this simulation, no noise is added to the signal.

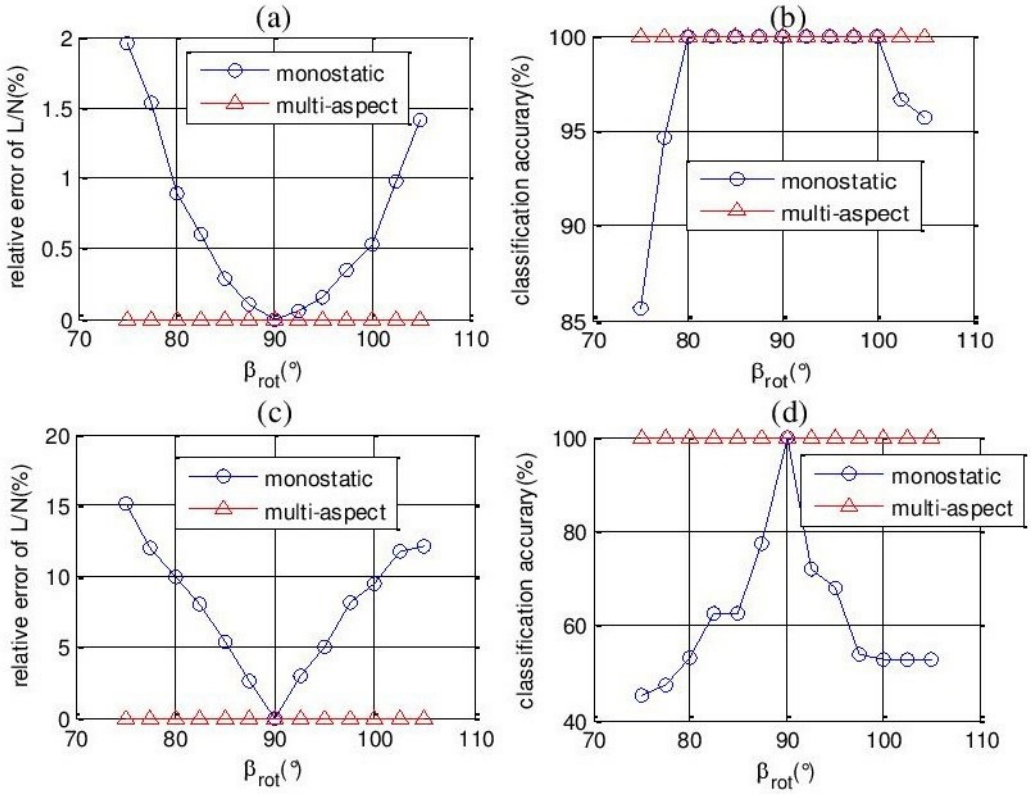

Fig. 5. *The performances of the proposed method and the monostatic algorithm under different helicopter attitudes.*
a The relative estimation error of L/N quotient versus angle β_{rot} when $\beta_{los,i} \in [0°, 3°]$.
b The classification accuracy versus angle β_{rot} when $\beta_{los,i} \in [0°, 3°]$.
c The relative estimation error of L/N quotient versus angle β_{rot} when $\beta_{los,i} \in [0°, 70°]$.
d The classification accuracy versus angle β_{rot} when $\beta_{los,i} \in [0°, 70°]$.

The averaged relative estimation error of L/N quotient and the classification accuracy versus β_{rot} are depicted in Fig. 5, respectively. In this paper, the classification accuracy is defined as the percentage of trials in which the helicopters are correctly classified. It is clear from Fig. 5 that the proposed method can accurately estimate the L/N quotient and successfully classify helicopters under each angle β_{rot} in both Scenario 1 and Scenario 2. In comparison, monostatic algorithm suffers different degrees of performance degradation in Scenarios 1 and 2. In Scenario 1, the estimation error of L/N quotient yielded by the monostatic algorithm is quite slight, and the classification accuracy of monostatic algorithm decreases mildly when β_{rot} deviates beyond [80°, 100°]. In Scenario 2, the performance of monostatic algorithm degrades obviously when β_{rot} deviates from 90°. Therefore, the proposed method have advantages over monostatic methods, especially when β_{rot} deviates obviously from 90° or the pitch angle of the LOS is not too small.

Allowing for that the deviation of angle β_{rot} from 90° can be as large as 30° for certain helicopter such as AH-64 Apache, and the LOS angles $\beta_{los,i}$ can be much larger than 3° in some applications [32], the multi-aspect deployment is justified in realistic scenarios.

4.2. The Performance of the Proposed Method in Noisy Conditions

In this simulation, the maximal Doppler $f_{md,max,i}$ and the period T_i are estimated in noisy conditions, and the performance of the proposed method is tested under different noise levels.

Table 6 The angle parameters in Simulation 4.2.

$\alpha_{los,i}$	randomly selected from [0°, 360°] with equal probability
$\beta_{los,i}$	Scenario 1: randomly selected from [0°, 3°] with equal probability Scenario 2: randomly selected from [0°, 70°] with equal probability
α_{rot}	randomly selected from [0°, 180°] with equal probability
β_{rot}	randomly selected from corresponding range stipulated in the pilot's handbook as depicted in Table 2

The carrier frequency f_c of radar is set to 900 MHz. The sampling frequency f_s and signal length M are set to be 6000 Hz and 2400 points, respectively. Six types of helicopters are considered and their parameters are listed in Table 2. The helicopter is observed from K (K=3 or 4) different aspects, the LOS angles ($\alpha_{los,i}$, $\beta_{los,i}$) and attitude angles (α_{rot}, β_{rot}) are randomly selected from their definition domains as depicted in Table 6. The SNR is set to vary from -5dB to 10dB with a step size of 5dB. Under each SNR, the algorithm is tested with 120 Monte Carlo trails.

The relative estimation error of L/N quotient and the classification accuracy are depicted in Fig. 6 (a) and (b), respectively. It is clear from Fig.6 that the proposed method outperforms monostatic algorithm in both Scenario 1 and Scenario 2 in noisy conditions, and the advantage of the proposed method over monostatic algorithm in Scenario 2 is larger than that in Scenario 1, which coincides with the observations in Section 4.1. It can be seen from Fig. 5 and Fig.6 that the advantage of the proposed method over monostatic algorithm in noisy conditions is larger than that in non-noise conditions in Scenario 1, which implies that the multi-aspect deployment has better robustness against noise than the monostatic deployment. In addition, the classification accuracy yielded by the proposed method with 4 observation aspects is higher than that yielded with 3 observation aspects.

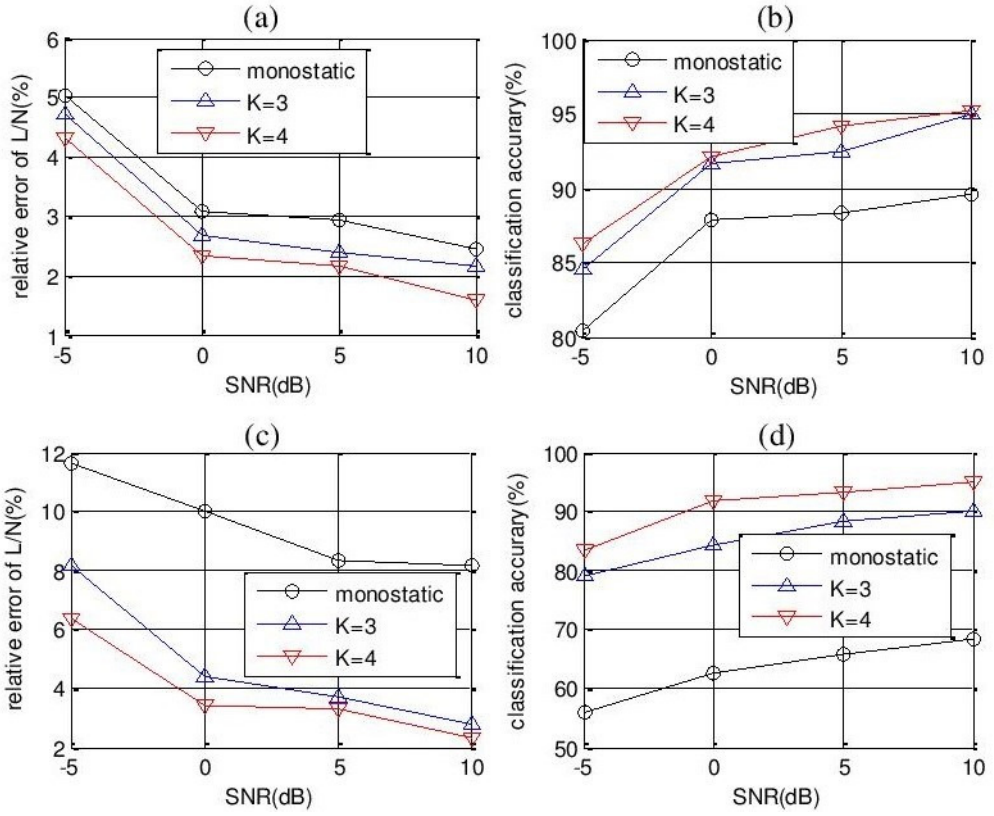

Fig. 6. *The performances of the proposed method under different noise levels.*
a The relative estimation error of L/N quotient versus SNR when $\beta_{los,i} \in [0°, 3°]$.
b The classification accuracy versus SNR when $\beta_{los,i} \in [0°, 3°]$.
c The relative estimation error of L/N quotient versus SNR when $\beta_{los,i} \in [0°, 70°]$.
d The classification accuracy versus SNR when $\beta_{los,i} \in [0°, 70°]$.

4.3. Experiments with Real Data

To illustrate the proposed algorithm, real echoes from a 5-blade rotor were recorded by a frequency modulated continuous wave (FMCW) radar at the carrier frequency of 9.8 GHz with a bandwidth of 200 MHz. The rotor is rotating without translation motion and its rotational speed and blade length are 5.5 revolutions per second (rps) and 0.18 m, respectively. The rotor attitude is non-horizontal, and the azimuth angle α_{rot} and pitch angle β_{rot} are approximately equal to 180° and 80°, respectively. In this experiment, the rotor is observed by this radar from multiple aspect angles, and the distance between the radar and the rotor is about 3 m. The pitch angles of the LOS are set much larger than 3° because we are aimed at applications of classifying micro-Drones in city scenarios. A diagram of the experiment setup is shown in Fig. 7 and the LOS angles are listed in Table 7.

The spectrograms of the received signals at Aspect 1, 2, and 3 are shown in Figs. 8 (a), (b) and (c), respectively. We can see that the maximal Doppler shifts in Fig. 8 (a), (b) and (c) are different from each other, which are estimated as 139 Hz, 167 Hz, and 222 Hz, respectively, using the method proposed in Section 3.1. It can be seen that the received signal is periodic, and period can be approximately

estimated as 36ms according to the spectrogram. Considered that the number of blades is 5, the rotational speed can be calculated as $\omega = 1/NT \approx 5.6$rps, which is approximately equal to the true value. It is worth emphasizing that the intensity of the positive Doppler shift of the received signal is much stronger than that of the negative Doppler shift, and the negative flashes of the received signal are almost buried in the noisy, this is because the scattering coefficients of the front side of the rotor blades are much larger than that of the rear side of the rotor blades.

Table 7 The LOS angles in real data experiment

	$\alpha_{los,i}$	$\beta_{los,i}$
Aspect 1	15°	60°
Aspect 2	45°	60°
Aspect 3	0°	45°

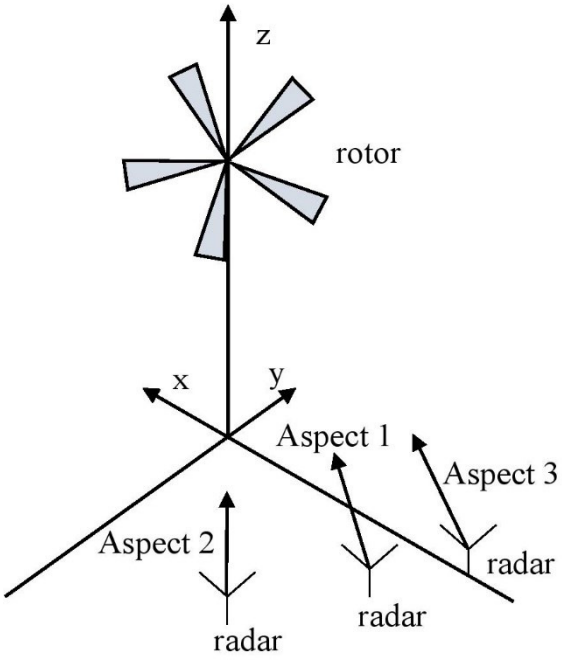

Fig. 7. *The setup of the real data experiment.*

With the estimated maximal Doppler shifts and the configurations of the LOS angles, the proposed algorithm is applied on the multi-aspect micro-Doppler signatures to determine the attitude angles and the *L*/*N* quotient. The resulted attitude angles are (171°, 79°), and the *L*/*N* quotient is estimated to be 0.0351, which is very close to the true value, i.e. 0.0360, with a relative error of 2.5%. The above results verify the effectiveness of the proposed method.

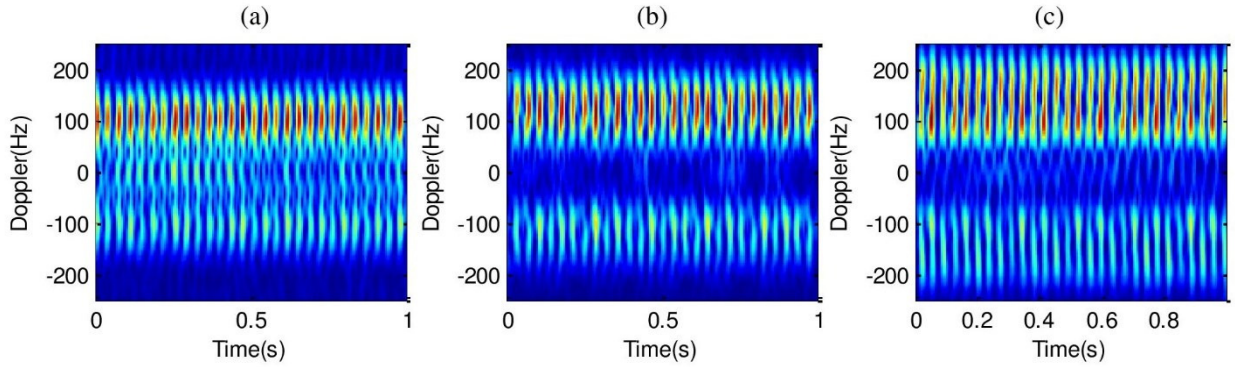

Fig. 8. *The spectrogram of the received signal from (a) Aspect1, (b) Aspect 2 and (c) Aspect 3.*

5. Conclusion

In this paper, an attitude-independent L/N quotient estimation algorithm is proposed based on multi-aspect micro-Doppler signatures. The proposed algorithm is robust to the helicopter attitude and capable of estimating the L/N quotients of non-horizontal helicopters. This algorithm has significant application in helicopter classification especially in conditions of non-cooperative targets with unknown attitudes. The proposed algorithm can be divided into two stages. First, the period and maximal Doppler shift of the received signal are extracted via monostatic micro-Doppler analysis at each aspect. Secondly, the attitude angles of the target are extracted via multi-aspect micro-Doppler analysis, and the L/N quotient is calculated by using the extracted attitude angles. The extracted L/N quotient can then be used in helicopter classification. Since the proposed algorithm accomplishes attitude-independent L/N quotient estimation, the accuracy of helicopter classification yielded by the proposed algorithm is higher than that yielded by the monostatic L/N quotient estimation methods. The performance gain of the proposed method is obtained at the cost of multi-aspect observations. In possible applications, a system using distributed MIMO with joint radar and communication capabilities as the one presented in [31] would allow a cost free sharing of the estimated maximal Doppler shift and periods, therefore, be capable of performing the proposed method without additional cost. It is worth emphasizing that the L/N quotient can be jointly used with other features such as range-slow-time image [16] to further improve the classification accuracy. The robustness of the proposed algorithm with respect to the helicopter attitude is evaluated with simulations. Experiments with real data have also confirmed the effectiveness of the proposed method.

6. Acknowledgments

This work was supported in part by the National Natural Science Foundation of China under Grants 61422110, 41271011 and 61661130158, and in part by the National Ten Thousand Talent Program of China (Young Top-Notch Talent), and in part by the Tsinghua National Laboratory for Information Science (TNList), and in part by the Tsinghua University Initiative Scientific Research Program.

7. References

[1] Chen, V. C., Li, F., Ho, S. S., *et al*.: 'Micro-Doppler effect in radar: phenomenon, model, and simulation study', IEEE Transactions on Aerospace and Electronic Systems, 2006, **42**, (1), pp. 2–21.

[2] Björklund, S., Petersson, H., Hendeby, G.: 'Features for micro-Doppler based activity classification', IET Radar, Sonar & Navigation, 2015, **9**, (9), pp. 1181–1187.

[3] Sparr, T., Krane, B.: 'Micro-Doppler analysis of vibrating targets in SAR', IEE Proceedings Radar, Sonar & Navigation, 2003, **150**, (4), pp. 277–283.

[4] Lei, J., and Lu, C.: 'Target classification based on micro-Doppler signatures', IEEE International Radar Conference, Arlington, USA, May 2015, pp. 179–183.

[5] Kim, Y., Ling, H.: 'Human activity classification based on micro-Doppler signatures using a support vector machine', IEEE Transactions on Geoscience and Remote Sensing, 2009, **47**, (5), pp. 1328–1337.

[6] Lei, P., Sun, J., Wang, J., *et al*.: 'Micromotion parameter estimation of free rigid targets based on radar micro-Doppler', IEEE Transactions on Geoscience and Remote Sensing, 2012, **50**, (10), pp. 3776–3786.

[7] Zhang, R., Li, G., Zhang, Y. D.: 'Micro-Doppler Interference Removal via Histogram Analysis in Time-Frequency Domain', IEEE Transactions on Aerospace and Electronic Systems, 2016, **52**, (2), pp. 755-768.

[8] Misiurewicz, J., Kulpa, K., Czekala, Z.: 'Analysis of radar echo from a helicopter rotor hub', in Proceedings of IEEE International Conference on Microwaves and Radar, 1998, no. 3, pp. 866–870.

[9] Thayaparan, T., Abrol, S., Riseborough, E., *et al*.: 'Analysis of radar micro-Doppler signatures from experimental helicopter and human data', IET Radar, Sonar and Navigation, 2007, **1**, (4), pp. 289–299.

[10] Rotander, C. E., Sydow, H. V.: 'Classification of helicopters by the L/N-quoutient', in Proceedings of the Radar 97, 1997, pp. 629–633.

[11] Muoz Ferraras, J., Perez Martinez, F., Burgos Garcia, M.: 'Helicopter classification with a high resolution LFMCW radar', IEEE Transactions on Aerospace and Electronic Systems, 2009, **45**, (4), pp. 1373–1384.

[12] Tikkinen, J. M., Helander, E., E., Visa, A.: 'Joint utilization of incoherently and coherently integrated radar signal in helicopter categorization', in IEEE International Radar Conference, Arlington, USA, May 2005, pp. 540–545.

[13] Costa, H., C., A., De Matos, M., C.: 'Measuring time between peaks in helicopter classification using continuous wavelet transform', in IEEE Radar Conference, Rome, Italy, May 2008, pp. 1–6.

[14] Oh, S. R., Pathak, K., Agrawal, S. K., *et al*.: 'Approaches for a tether-guided landing of an autonomous helicopter', IEEE Transactions on Robotics, 2006, **22**, (3), pp. 536–544.

[15] Barczyk, M., Lynch, A. F.: 'Invariant observer design for a helicopter UAV aided inertial navigation system', IEEE Transactions on Control Systems Technology, 2013, **21**, (3), pp. 791–806.

[16] Yoon, S. H., Kim, B., Kim, Y. S.: 'Helicopter classification using time-frequency analysis', IET Electronics Letters, 2000, **36**, (22), pp. 1871–1872.

[17] Zhang, R., Li, G., Clemente, C., *et al*.: 'Helicopter classification via period estimation and time-frequency masks', In IEEE 6th International Workshop on Computational Advances in Multi-Sensor Adaptive Processing, Cancun, Mexico, Dec. 2015, pp. 61–64.

[18] Setlur, P., Ahmad, F., Amin, M.: 'Helicopter radar return analysis: Estimation and blade number selection', Signal Processing, 2011, **91**, (6), pp. 1409–1424.

[19] Gaglione, D., Clemente, C., Coutts, F., *et al*.: 'Model-based sparse recovery method for automatic classification of helicopters', In 2015 IEEE Radar Conference, Johannesburg, South Africa, Oct. 2015, pp. 1161–1165.

[20] Zhu, R. F., Zhang, Q., Zhu, X. P., *et al*.: 'Micro-Doppler analysis of vibrating target in bistatic radar', In 2nd Asian-Pacific Conference on Synthetic Aperture Radar, Xian, China, Oct. 2009, pp. 981–984.

[21] Luo, Y., He, J., Liang, X. J., *et al*.: 'Three-dimensional micro-Doppler signature extraction in MIMO radar', In 2nd International Conference on Signal Processing Systems, Dalian, China, Feb. 2010, pp. V2–1.

[22] Clemente, C., Soraghan, J. J.: 'Vibrating target micro-Doppler signature in bistatic SAR with a fixed receiver', IEEE Transactions on Geoscience and Remote Sensing, 2012, **50**, (8), pp. 3219–3227.

[23] Smith, G. E., Woodbridge, K., Baker, C. J., *et al*.: 'Multistatic micro-Doppler radar signatures of personnel targets', IET Signal Processing, 2010, **4**, (3), pp. 224–233.

[24] Karabacak, C., Gürbüz, S. Z., Guldogan, M. B., *et al*.: 'Multi-aspect angle classification of human radar signatures', Proceedings of SPIE, 2013, pp. 873408–873408.

[25] Fioranelli, F., Ritchie, M., Griffiths, H.: 'Multistatic human micro-Doppler classification of armed/unarmed personnel', IET Radar, Sonar & Navigation, 2015, **9**, (7), pp. 857–865.

[26] Fairchild, D. P., Narayanan, R. M.: 'Multistatic micro-doppler radar for determining target orientation and activity classification', in IEEE Transactions on Aerospace and Electronic Systems, 2016, **52**, (1), pp. 512–521.

[27] Clemente, C., Soraghan, J. J., 'GNSS-based passive bistatic radar for micro-Doppler analysis of helicopter rotor blades', IEEE Transactions on Aerospace and Electronic Systems, 2014, **50**, (1), 491–500.

[28] Frankford, M. T., Stewart, K. B., Majurec, N., *et al*.: 'Numerical and experimental studies of target detection with MIMO radar', IEEE Transactions on Aerospace and Electronic Systems, 2014, **50**, (2), pp. 1569–1577.

[29] Baczyk, M. K., Samczyński, P., Kulpa, K., *et al*.: 'Micro-Doppler signatures of helicopters in multistatic passive radars', IET Radar, Sonar & Navigation, 2015, **9**, (9), pp. 1276–1283.

[30] Gu, J. F., Zhu, W. P., Swamy, M. N. S.: 'Joint 2-D DOA estimation via sparse L-shaped array', IEEE Transactions on Signal Processing, 2015, **63**, (5), pp. 1171–1182.

[31] Gaglione, D., Clemente, C., Ilioudis, C. V., *et al*.: 'Fractional Fourier Based Waveform for a Joint Radar-Communication System', in IEEE International Radar Conference 2016, Philadelphia, USA, May 2016, pp. 2–16.

[32] Ritchie, M., Fioranelli, F., Borrion, H., & Griffiths, H.: 'Multistatic micro-doppler radar feature extraction for classification of unloaded/loaded micro-drones'. IET Radar, Sonar and Navigation, 2016.